



OPEN ACCESS

EDITED BY

Åke Sjöholm,
Gävle Hospital, Sweden

REVIEWED BY

Ivan Torre-Villalvazo,
Instituto Nacional de Ciencias Médicas
y Nutrición Salvador Zubirán
(INCMNSZ), Mexico

Raquel Soares,
University of Porto, Portugal
Ariane Zamoner,
Federal University of Santa Catarina,
Brazil

*CORRESPONDENCE

Maria Paula Macedo
paula.macedo@nms.unl.pt

SPECIALTY SECTION

This article was submitted to
Clinical Diabetes,
a section of the journal
Frontiers in Endocrinology

RECEIVED 17 March 2022

ACCEPTED 12 July 2022

PUBLISHED 17 August 2022

CITATION

Meneses MJ, Sousa-Lima I, Jarak I,
Raposo JF, Alves MG and Macedo MP
(2022) Distinct impacts of fat and
fructose on the liver, muscle, and
adipose tissue metabolome: An
integrated view.
Front. Endocrinol. 13:898471.
doi: 10.3389/fendo.2022.898471

COPYRIGHT

© 2022 Meneses, Sousa-Lima, Jarak,
Raposo, Alves and Macedo. This is an
open-access article distributed under
the terms of the [Creative Commons
Attribution License \(CC BY\)](https://creativecommons.org/licenses/by/4.0/). The use,
distribution or reproduction in other
forums is permitted, provided the
original author(s) and the copyright
owner(s) are credited and that the
original publication in this journal is
cited, in accordance with accepted
academic practice. No use,
distribution or reproduction is
permitted which does not comply with
these terms.

Distinct impacts of fat and fructose on the liver, muscle, and adipose tissue metabolome: An integrated view

Maria João Meneses^{1,2}, Inês Sousa-Lima¹,
Ivana Jarak^{3,4}, João F. Raposo^{1,2}, Marco G. Alves⁵
and Maria Paula Macedo^{1,2,5*}

¹NOVA4Health, NOVA Medical School/Faculdade de Ciências Médicas (NMS/FCM), Universidade Nova de Lisboa, Lisbon, Portugal, ²Portuguese Diabetes Association - Education and Research Center (APDP-ERC), Lisbon, Portugal, ³Department of Pharmaceutical Technology, Faculty of Pharmacy, University of Coimbra, Coimbra, Portugal, ⁴Department of Anatomy and Unit for Multidisciplinary Research in Biomedicine (UMIB), Institute of Biomedical Sciences Abel Salazar (ICBAS), University of Porto, Porto, Portugal, ⁵Medical Sciences Department, University of Aveiro, Aveiro, Portugal

Objective: In the last years, changes in dietary habits have contributed to the increasing prevalence of metabolic disorders, such as non-alcoholic fatty liver disease (NAFLD) and type 2 diabetes mellitus (T2DM). The differential burden of lipids and fructose on distinct organs needs to be unveiled. Herein, we hypothesized that high-fat and high-fructose diets differentially affect the metabolome of insulin-sensitive organs such as the liver, muscle, and different adipose tissue depots.

Methods: We have studied the impact of 12 weeks of a control (11.50% calories from fat, 26.93% from protein, and 61.57% from carbohydrates), high-fat/sucrose (HFat), or high-fructose (HFruet) feeding on C57Bl/6J male mice. Besides glucose homeostasis, we analyzed the hepatic levels of glucose and lipid-metabolism-related genes and the metabolome of the liver, the muscle, and white (WAT) and brown adipose tissue (BAT) depots.

Results: HFat diet led to a more profound impact on hepatic glucose and lipid metabolism than HFruet, with mice presenting glucose intolerance, increased saturated fatty acids, and no glycogen pool, yet both HFat and HFruet presented hepatic insulin resistance. HFat diet promoted a decrease in glucose and lactate pools in the muscle and an increase in glutamate levels. While HFat had alterations in BAT metabolites that indicate increased thermogenesis, HFruet led to an increase in betaine, a protective metabolite against fructose-induced inflammation.

Conclusions: Our data illustrate that HFat and HFruct have a negative but distinct impact on the metabolome of the liver, muscle, WAT, and BAT.

KEYWORDS

prediabetes, non-alcoholic fatty liver disease, diet, metabolomics, muscle, adipose tissue

Introduction

Dysmetabolism drives obesity and/or diabetes as a result of excessive and abnormal accumulation of body fat impinging on several adverse health effects (1). Although awareness for these health and social problems has increased over the years, its prevalence continues to increase dramatically (2). Genetic background influences dysmetabolism development (3), yet the vast majority of the cases are due to factors that arose in industrialized countries, namely, excessive consumption of highly processed and energy-dense foods, frequently combined with a sedentary lifestyle. Indeed, these diets are usually rich in fructose and fat. While fructose is known to promote hepatic *de novo* lipogenesis, lipid accumulation, and insulin resistance (4), high-fat diets lead not only to hepatic lipid accumulation but also to higher adipose tissue lipolysis (5). However, fats and specifically triglycerides are differently metabolized depending on the fatty acid chain length. While medium-chain triglycerides are absorbed into the portal circulation and transported to the liver, long-chain fatty acids are transported through the lymphatic system *via* chylomicrons (6).

The metabolic and homeostatic dysfunctions (7) caused by the poor lifestyle habits may end up in the onset of hypertension, type 2 diabetes mellitus (T2DM) (8), cardiovascular disease, dyslipidemia (9), and non-alcoholic fatty liver disease (NAFLD) (10). The latter is characterized by the presence of macrovesicular steatosis in $\geq 5\%$ of hepatocytes, in individuals with no causes for secondary hepatic accumulation, as is the case of abusive alcohol consumption and hereditary disorders (11). NAFLD is the most common cause of chronic liver disease in Western countries, having a reported prevalence of 6%–35% worldwide (12). Although the molecular mechanisms leading to NAFLD are still under discussion, it is known that it is a consequence of several factors, namely, (i) an increased incursion of free fatty acids from insulin-resistant adipose tissue, (ii) impaired metabolism of dietary lipids in the liver or impaired lipid export from the hepatocytes, and (iii) increased *de novo* lipogenesis in the liver (13). The overload of lipids affects not only the liver but also other metabolic organs such as the muscle or adipose tissue (both white and brown). Considering organ crosstalk, dysfunctions in one of these organs will have an impact on others, namely, in cases of insulin resistance and inflammation, and dysmetabolism overall (14, 15).

We hypothesized that dietary content in lipids or fructose differentially affect the metabolome of insulin-sensitive organs. Our aim was to evaluate the metabolome of insulin-sensitive organs, as is the case of the liver, muscle, and white and brown adipose tissue in animals fed with high-fat or high-fructose diet.

Materials and methods

Chemicals

Bicinchoninic acid (BCA) Protein Assay Kit was purchased from Thermo Scientific (Waltham, MA, USA). Dried milk was purchased from Nestlé (Vevey, Switzerland). Amersham ECL was purchased from GE Healthcare (Weßling, Germany). NZYColour Protein Marker II, agarose, NZYDNA Ladder V, and Supreme NZYTaQ II 2x Green Master Mix were purchased from NZYTech (Lisbon, Portugal). Fructose was purchased from Enzymatic (Loures, Portugal). Immobilon-P polyvinylidene difluoride (PVDF) membrane was purchased from Merck Millipore (MA, USA). Kits for triglycerides and cholesterol determination were purchased from Spinreact (Girona, Spain). Quantification of free fatty acids was done using a kit from Wako Diagnostics (CA, USA). All other chemicals were purchased from Sigma-Aldrich (St. Louis, MO, USA), unless stated otherwise.

Animals

Experiments were performed using male C57Bl6/J mice kept on a 12-h light/dark cycle with *ad libitum* access to food and water. Animals were randomly divided in three groups ($n=7$ /group) and fed different diets from 6 to 18 weeks of age: normal chow diet with 11.50% calories from fat, 26.93% from protein, and 61.57% from carbohydrates [Chow group; RM3A(P), Special Diets Services, Witham, Essex, UK]; high-fat diet with 58% of calories from fat, 16.4% from protein, and 25.5% from carbohydrates (HFat; D12331, Research Diets, New Brunswick, NJ) or high fructose diet [HFruct; FRUC-00T-500, Enzymatic, PT; 35% w/v in drinking water and fed with RM3A(P) diet]. Mice were monitored weekly for body weight, blood glucose levels, and for distress signals. The experimental procedures

were approved by the Ethics Committee of the NOVA Medical School and by the Directorate-General for Food and Veterinary that regulates the animal care and use in research (registration number 82/2019/CEFCM and 0421/000/000/2016, respectively). All procedures followed Animal Research: Reporting of *In Vivo* Experiments (ARRIVE) guidelines and the European laws (Directive 2010/63/EU) that rule the use of animals in research.

Metabolic measurements

Mice were weighed at 6 weeks and weekly thereafter. Blood glucose levels were measured using a Contour Next glucose meter (Bayer, Leverkusen, Germany). Food and caloric intake were also assessed. For glucose tolerance tests, mice were fasted overnight at 17 weeks of age, and blood glucose levels were measured before and 15, 30, 60, 90, and 120 min after intraperitoneal injection of glucose (2.0 g/kg). The area under the curve (AUC) was calculated using the trapezoidal rule for glucose data (16). For insulin tolerance tests, at 17 weeks of age, mice were fasted for 5 h, and blood glucose levels were measured before and 15, 30, 60, 90, and 120 min after intraperitoneal injection of human insulin (0.75 UI/Kg; Actrapid, Novo Nordisk).

Insulin signaling studies

Mice were fasted overnight and intraperitoneally injected with human insulin (10 UI/kg of body weight; Actrapid, Novo Nordisk) or saline and sacrificed 10 min later. Organs [liver, epididymal white adipose tissue (WAT), interscapular brown adipose tissue (BAT), and gastrocnemius muscle] were harvested, snap frozen, and stored at -80°C until analysis. The liver was homogenized in lysis buffer (in mM: 20 Tris pH 7.5, 5 EDTA, 10 $\text{Na}_4\text{P}_2\text{O}_7$, 100 NaF, 2 Na_3VO_4) with 1% NP-40 and protease inhibitors (Roche, Switzerland). Tissue lysates (20 μg protein) were mixed with Laemmli sample buffer (in %: 1.5 Tris, 20 glycerol, 4.1 SDS, 2 β -mercaptoethanol, 0.02 bromophenol blue, pH 6.8) and denatured for 10 min at 95°C . Proteins were fractionated in 10% polyacrylamide gels. The proteins were transferred from gels to previously activated PVDF membranes in TransBlot Turbo (Bio-Rad Laboratories, Hemel Hempstead, UK) and then blocked for 1 h in a 5% non-fat milk solution at room temperature. The membranes were incubated overnight at 4°C with the primary antibodies listed in [Supplementary Table S1](#) and incubated with secondary antibodies for 1 h. Either glyceraldehyde 3-phosphate dehydrogenase (GAPDH) or β -actin were used as loading controls. Membranes were reacted with Amersham ECL Prime Western Blotting Detection Reagent (GE Healthcare), read in Chemidoc, and quantified using ImageLab (Bio-Rad Laboratories).

Liver histology and lipid assay

Liver was fixed with 10% formalin solution, embedded in paraffin, and cut in $4\text{-}\mu\text{m}$ sections. These sections were then stained with hematoxylin and eosin for the characterization of liver morphology and lipid content. Hepatic lipids were extracted as previously described (17). Briefly, approximately 250 mg of frozen tissue was rapidly mixed with high-performance liquid chromatography (HPLC)-grade methanol (4.6 ml/g) followed by methyl-tert-butyl ether (MTBE) (15.4 ml/g). The mixture was placed in a shaker for 4 h and then centrifuged at $13,000g$ for 10 min. The liquid fraction was collected, and phase separation was induced by adding 1 ml of distilled water and letting it rest at room temperature for 10 min. The liquid was then centrifuged for 10 min at $1,000g$. The organic phase, containing the lipids, was separated and dried under nitrogen gas in a glass vial protected from light. It was then dissolved in butanol:(Triton X-100:methanol). Hepatic total cholesterol and triglyceride contents were determined by enzymatic method (SpinReact).

Quantitative real-time polymerase chain reaction

The extraction of liver total ribonucleic acid (RNA) was performed using TRIzol (Invitrogen), and the concentrations were determined by a Nanodrop 2000 spectrophotometer (Thermo Fisher Scientific). Total RNA was reverse transcribed to complementary DNA (cDNA) using high-capacity cDNA reverse transcription kit (Applied Biosystems, CA, USA). Quantitative real-time polymerase chain reaction (qPCR) was performed to evaluate the abundance of messenger RNA (mRNA) coding for GK, G6Pase, PEPCK, ChREBP, SREBP2, ELOVL2, CD36, SCD1, β -actin, and β -2-microglobulin using SYBRTM Green PCR Master Mix (Applied Biosystems) in an ABI 7500 (Applied Biosystems). Specific exon-exon spanning primers were designed for the amplification of the target and housekeeping transcripts ([Supplementary Table S2](#)). β -Actin and β -2-microglobulin transcript levels were used to normalize gene expression levels. Fold variation in gene expression levels was calculated with the $2^{-\Delta\Delta\text{Ct}}$ method (18).

Metabolite extraction

To extract the liver, gastrocnemius muscle, epididymal WAT, and interscapular BAT metabolites, the different tissues were homogenized in glass vials using a mixture of methanol and chloroform (2:1). After sonication on ice for 15 min, chloroform and water (1:1) were added, and samples were centrifuged at $10,000g$ for 15 min at 4°C . Polar and apolar fractions were

isolated and evaporated using a flow of nitrogen. The polar fraction was dissolved in D₂O phosphate buffer (0.2 M, pH 7) for proton nuclear magnetic resonance (¹H-NMR) analysis.

Proton nuclear magnetic resonance spectroscopy

Proton nuclear magnetic resonance (¹H-NMR) spectra of the polar extracts were acquired using a Varian Inova 600 MHz (14.1 T) spectrometer equipped with a 3-mm QXI probe with a z-gradient. ¹H-1D NOESY experiments with water presaturation were acquired at 298 K (7.2 kHz spectral width, 0.1 s mixing time, four dummy scans, 4 s relaxation delay with 3 s of water presaturation, 90°C pulse angle, 3 s acquisition time, and a minimum of 128 scans). For further spectral assignment, two-dimensional spectra (TOCSY) were acquired using sweep width of 5.4 kHz in both dimensions, 48 transients, and 400 and 1,024 points in t1 and t2 dimensions, respectively. Spectra were treated by multiplying FIDs with exponential window function (line broadening of 0.3 Hz) and were zero filled to 64 k points prior to Fourier transformation using TopSpin (Bruker Biospin, Karlsruhe, Germany). 2D spectra were processed by applying q sine window function and zero filled to 2,048 points in both dimensions. The comparison of 1D and 2D spectra with reference spectra and public databases such as HMDB allowed for peak assignment and metabolite identification (19). Metabolites were identified according to metabolomics standards initiative guidelines for metabolite identification (20).

Multivariate analysis of NMR data

Processed 1D NOESY spectra were bucketed using one-point bucket (0.6–9.0 ppm, with signal-free, water, and fumarate regions excluded). Data matrix was built in Amix Viewer (BrukerBiospin, Rheinstetten). Icoshift algorithm (21) was used to align bucketed spectra, and total area integral normalization was applied to account for the variations in the overall sample concentrations. Multivariate statistical analysis was applied on unit variance scaled matrix (SIMCA 14, Umetrics, Sweden). Principal component analysis (PCA) was used to provide information on global data structure, and partial least squares discriminant analysis (PLS-DA) was used to assess group separation and to identify the main metabolites that contribute to the group discrimination. PLS-DA models were validated by sevenfold cross-validation and permutation test (n=100) to provide the qualitative measure of predictive power (Q₂) and to assess the degree of fit to the data (R₂). The corresponding PLS-DA loadings were obtained by multiplying the loading weight factors (w) by the standard deviation of the respective variable and were color-coded according to variable

importance in the projection (VIP). All differentially expressed metabolites for each of the diets in each tissue were used to identify the most relevant metabolic pathways affected by diet using MetaboAnalyst (22).

GC-MS analysis

Fatty acid methyl esters were obtained by base-catalyzed transmethylation (2 M KOH in methanol). The resultant fatty acid methyl ester solution was analyzed by gas chromatography using a Shimadzu GC-MS QP2010 UltraGas Chromatograph Mass Spectrometer (Shimadzu, Kyoto, Japan), with a capillary column BPX70 (0.25 mm internal diameter, 0.25 μm film thickness, 30 m long, SGE, Austin, TX, USA). Nonadecanoic fatty acid (C19:0) was used as the internal standard. The injector temperature was set at 250°C, and 1 μl of each sample was injected with a split ratio of 1:80. Helium was used as the carrier gas. The initial column temperature was 155°C, followed by a heating rate of 1°C/min up to 170°C, 4°C/min up to 220°C and 40°C/min until reaching 250°C, which was kept for 5 min. The linear velocity was 35 cm/s, with interface temperature of 250°C, ion source temperature of 225°C, mass range of 45–500, and event time of 0.3 s. All the measurements were repeated three times, and the average values were reported. Fatty acids were identified by retention time and fragmentation profile and quantified by the internal standard procedure. Results are expressed as a percentage of total fatty acids.

Statistical analysis

Experimental data are shown as mean ± standard error of mean (SEM). Unless stated otherwise, statistical analysis was performed using one-way ANOVA in GraphPad Prism 8 (GraphPad Software, San Diego, CA, USA). p<0.05 was considered significant.

Results

HFat diet-fed mice develop glucose intolerance, insulin resistance, and non-alcoholic fatty liver disease

Mice were subjected to a Chow, HFat, or HFruet diet. After a 12-week period of diet intervention, mice subjected to an HFat diet had increased body weight gain (37.90 ± 1.06 g) compared to Chow-diet-fed mice (28.14 ± 0.57 g; Figure 1A). Conversely, HFruet-diet-fed mice had decreased body weight (24.86 ± 0.76 g). In fact, after 12 weeks of diet, HFat-diet-fed

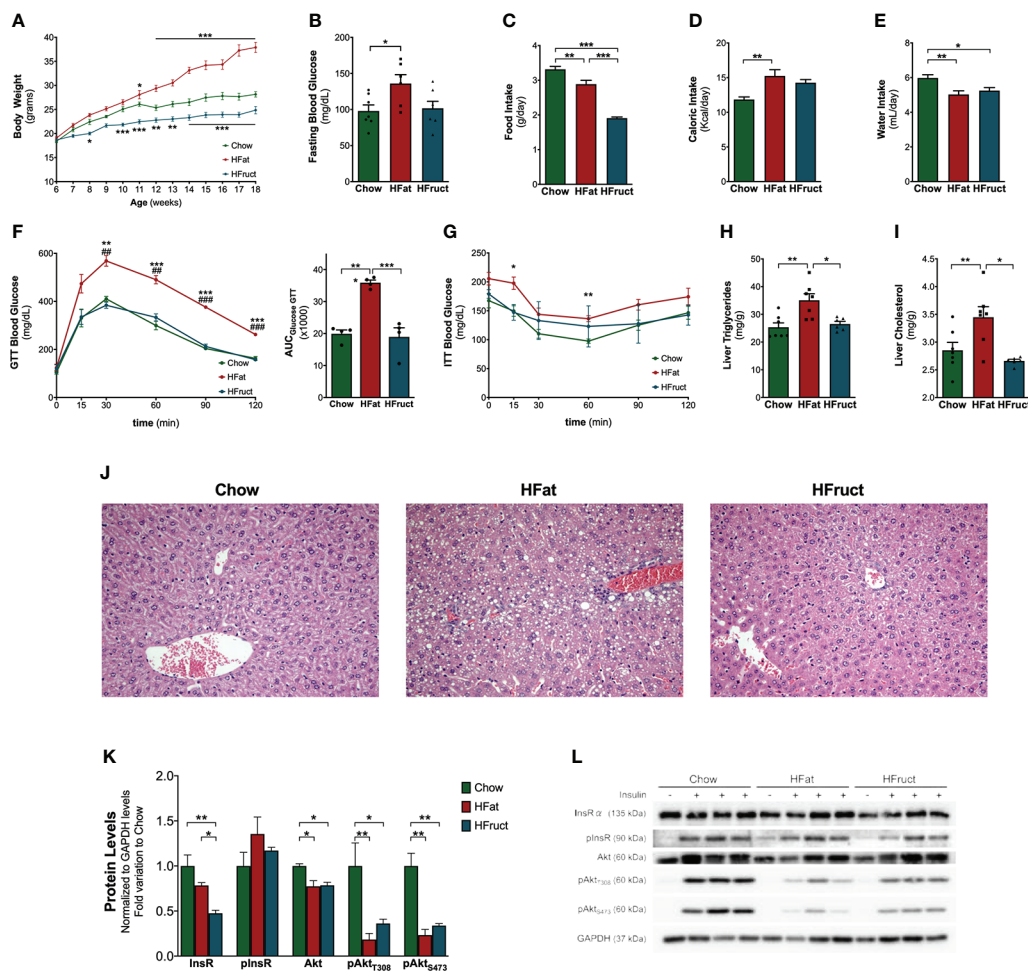


FIGURE 1
 Effects of HFat and HFruce diets on metabolic parameters, glucose homeostasis, hepatic lipid deposition, and insulin signaling pathway in C57Bl/6J male mice. (A) Body weight, (B) intraperitoneal glucose tolerance test (ipGTT) and the respective area under the curve (AUC), (C) insulin tolerance test (ITT); (D) fasting blood glucose; (E) food intake; (F) water intake; (G) caloric intake; (H) hepatic triglycerides; (I) hepatic cholesterol levels; (J) representative images of hematoxylin and eosin-stained liver sections; (K) Chow, high-fat (HFat) and high-fructose (HFruce) hepatic protein levels of insulin receptor α (InsR), phosphorylated-insulin receptor (pInsR; normalized to InsR levels); protein kinase B (PKB/Akt) and its phosphorylation sites (pAkt₃₀₈ and pAkt₄₇₃; normalized to Akt levels) normalized to GAPDH levels and represented as fold variation to Chow group; (L) representative images of Western blot for the described antibodies. Data are presented as mean \pm SEM for three to seven mice. * $p < 0.05$, ** $p < 0.01$, *** $p < 0.001$; (F) ## $p < 0.01$ vs. HFruce, ### $p < 0.001$ vs. HFruce.

mice had marked hyperglycemia (136 \pm 12 mg/dl), compared to Chow-diet-fed mice (98 \pm 8 mg/dl, **Figure 1B**), while HFruce-diet-fed mice were normoglycemic (102 \pm 10 mg/dl). HFruce-diet-fed mice had decreased water intake, concomitant with decreased food intake, compared to Chow-diet-fed mice. However, this was not reflected in a decrease in caloric intake (**Figures 1C–E**). Caloric intake was increased by 25% in HFat-diet-fed mice, compared to Chow-diet-fed mice (**Figure 1D**). HFat-diet-fed mice were glucose intolerant, as observed by failure to decrease blood glucose levels after administration of a glucose bolus (**Figure 1F**). HFruce-diet-fed mice displayed normal glucose tolerance, but the ITT curve was flatter than

Chow, revealing insulin resistance, as the capacity to decrease blood glucose levels after an insulin bolus is compromised (**Figures 1F, G**).

Dysmetabolism is associated with ectopic fat deposition in parenchymatous organs such as the liver. To evaluate this, hepatic triglycerides and cholesterol were measured. Liver content in both triglycerides and cholesterol was increased in HFat-diet-fed mice (35.1 \pm 2.3 mg/g and 3.5 \pm 0.2 mg/g, respectively) but unchanged in HFruce-diet-fed mice (26.5 \pm 0.9 mg/g and 2.7 \pm 0.03 mg/g, respectively; **Figures 1H, I**) when compared with Chow-diet-fed mice (25.4 \pm 1.6 mg/g and 2.9 \pm 0.1 mg/g, respectively). The

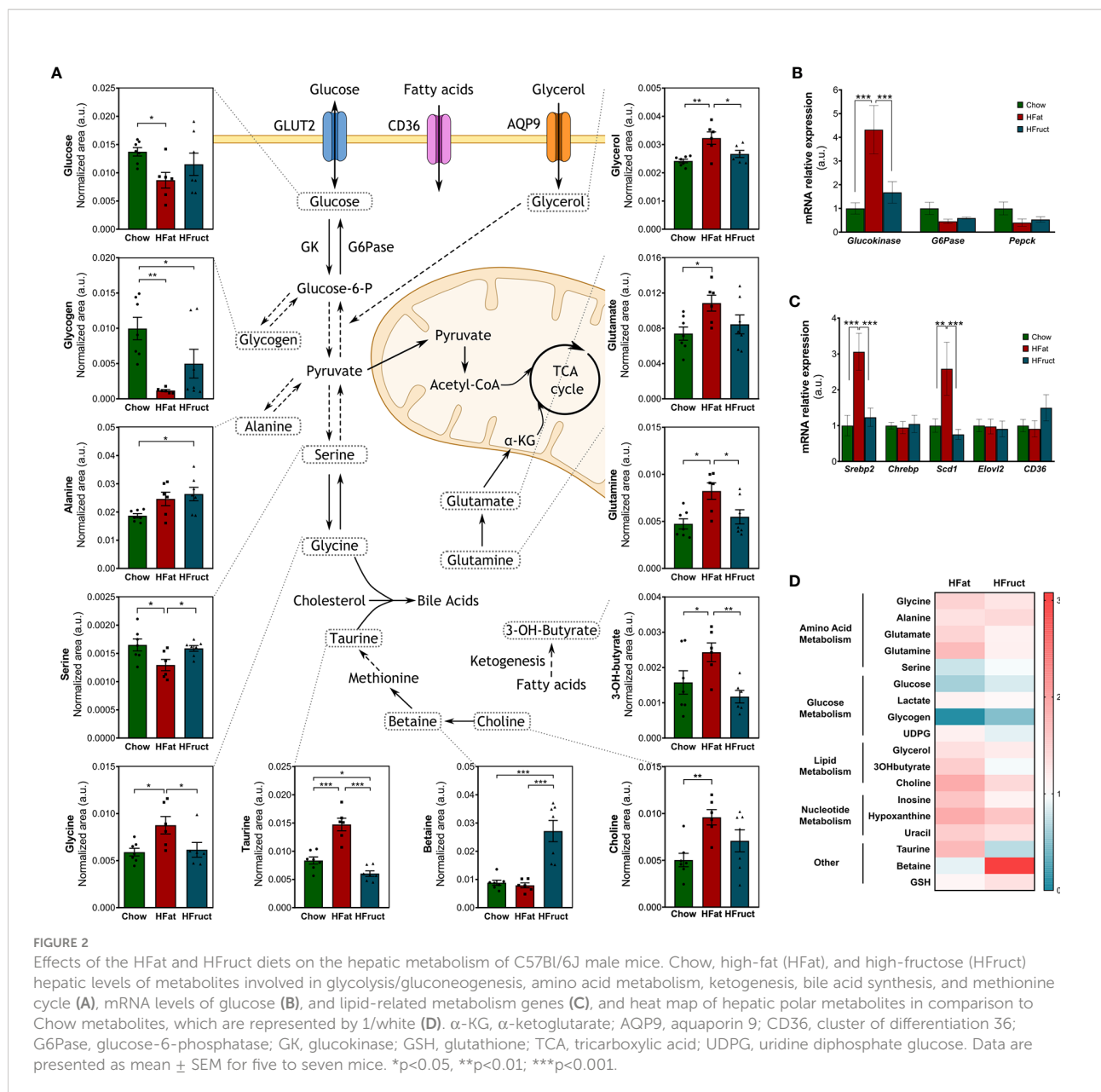
analysis of histological sections demonstrated that HFat-diet-fed mice developed NAFL, i.e., presented lipid droplets in >5% of the sections, whereas HFruct-diet-fed mice had mild hepatic degeneration (Figure 1J). Insulin-stimulated glucose utilization relies on an effective insulin signaling and is known to impact the transcription of several lipid and carbohydrate metabolism-related genes (23). Therefore, the protein levels of the insulin pathway-related components, insulin receptor (InsR) and Akt, in the liver of the mice were determined. After 12 weeks of diet exposure, HFruct-diet-fed mice presented a decrease in InsR α levels. However, the activation of the pathway, observed by the ratio between phosphorylated-insulin receptor (pInsR) and InsR, did not present any differences between the groups, suggesting that InsR are functional (Figures 1K, L). When analyzing Akt phosphorylation levels, there was a marked reduction in both T308 and S473 in both HFat- and HFruct-diet-fed groups, revealing that both diets negatively impact on the activation of the insulin signaling pathway (Figures 1K, L).

Hepatic carbohydrate and lipid and amino acid metabolisms are impaired by HFat and HFruct diets

The liver is a key organ for the maintenance of normal glucose homeostasis. However, this homeostasis is impaired in insulin-resistant states; thus, we evaluated the intracellular levels of key metabolites in the fasting state, and the mRNA expression of some glucose metabolism-related genes. Intra-hepatic glucose levels were decreased in HFat-diet-fed mice compared to Chow-diet-fed mice (Figure 2A). The mRNA levels of glucokinase, the enzyme responsible for the conversion of glucose into glucose-6-phosphate, thus enabling the trapping of glucose inside the cells, are increased in HFat-diet-fed mice (4.32 \pm 1.02-fold variation to Chow), when compared to both Chow- and HFruct-diet-fed mice (1.00 \pm 0.24- and 1.68 \pm 0.45-fold variation to Chow, respectively; Figure 2B). The mRNA expression of glucose-6-phosphatase, the enzyme that converts glucose-6-phosphate to glucose, does not present any significant difference between the groups, although there is a decrease in the HFat group, when compared to Chow (0.45 \pm 0.09- and 1.00 \pm 0.26-fold variation to Chow, respectively; $p=0.06$; Figure 2B). The expression of *Pepck*, responsible for glucose production from pyruvate, was also analyzed, although no statistical differences were found. In the fasting state, the liver produces glucose from several substrates, namely, glycogen. However, we observed that both HFat- and HFruct-diet-fed mice present lower levels of glycogen in the liver when compared to Chow-diet-fed mice. Glucose may also enter glycolysis to yield pyruvate; the latter has three major outcomes, namely, acetyl-CoA, acetate, or lactate. However, we observed that hepatic lactate and acetate levels do not vary significantly with the diet (data not shown).

Like for carbohydrates, the liver is essential for fatty acid metabolism. Dysregulations in cholesterol biosynthesis or *de novo* lipogenesis, in a key lipogenic tissue as the liver, may disrupt the overall lipid homeostasis. Thus, we evaluated intracellular levels of key metabolites for lipid metabolism and the mRNA expression of some lipid-metabolism-related genes. No statistical differences were found regarding *CD36* mRNA levels nor *Elovl2*, responsible for the elongation. However, *Srebp2* and *Scd1* mRNA levels were increased in HFat-diet-fed mice (3.06 \pm 0.51- and 2.59 \pm 0.74-fold variation to Chow; Figure 2C), when compared to both Chow (1.00 \pm 0.29- and 1.00 \pm 0.19-fold variation to Chow) and HFruct groups (1.23 \pm 0.26- and 0.76 \pm 0.14-fold variation to Chow; Figure 2C). Glycerol, a product of adipose tissue lipolysis, is an important substrate for both gluconeogenesis and lipogenesis (24). Glycerol levels were increased in the liver of HFat-diet-fed mice, when compared to Chow-diet-fed mice. Choline, which is the precursor for the essential component of the very low density lipoprotein (VLDL) phosphatidylcholine, was increased in HFat-diet-fed mice, compared to Chow-diet-fed mice (Figure 2A). Choline is oxidized to betaine, an osmoregulator and a methyl-group donor (25). Betaine was increased in HFruct-fed-mice compared to both Chow- and HFat-fed mice (Figure 2A). When glycogen is not available to produce glucose as energy substrate, ketogenesis takes place. One of the metabolites produced during this process is 3-hydroxybutyrate, which was increased in HFat-diet-fed mice, when compared to Chow- and HFruct-diet-fed animals (Figure 2A).

Besides being the basic units for protein synthesis, amino acids serve as intermediate metabolites for TCA cycle and lipid and nucleotide biosynthesis and sustain cell proliferation. Amino acid levels were significantly altered in the liver tissue by both high-fat and high-fructose diets. Serine, besides being a precursor of proteins and lipids, is involved in glycogen storage in the liver (26). Its levels were decreased in HFat-diet-fed mice, when compared to both Chow- and HFruct-diet-fed animals (Figure 2A). Serine is inter-convertible with glycine (27). The levels of this amino acid were increased in ~50% in the HFat group, when compared with both Chow- and HFruct-diet-fed mice (Figure 2A). During fasting, alanine participates in gluconeogenesis. Alanine levels were increased in almost 40% in HFruct mice when compared to Chow-diet-fed mice (Figure 2A). α -Ketoglutarate (α -KG), one of the metabolites of the Krebs cycle, may be interconverted into glutamate, which may be, in turn, interconverted in glutamine, an important amino acid and a precursor for gluconeogenesis and glutathione synthesis (28). Both glutamate and glutamine were increased in HFat-diet-fed mice when compared to Chow-diet-fed animals (Figure 2A). A graphical diagram with the most affected metabolites is depicted in Figure 2A, along with the graphs for each metabolite and a heat map (Figure 2D); the most affected pathways in the liver by HFat or HFruct feeding is shown in Supplementary Figures 1A, B, respectively.



HFat and HFruet diets increase hepatic monounsaturated fatty acids and decrease n-6 polyunsaturated fatty acids

As previously mentioned, the liver is a key lipogenic tissue; thus, fatty acid methyl esters levels were analyzed upon HFat and HFruet feeding for 12 weeks. After grouping fatty acids by saturation degrees, we observed that HFat diet leads to an increase in relative abundance of monounsaturated fatty acids (MUFA; 45.60 ± 1.61) when compared to Chow-fed mice (27.91 ± 1.13 ; Table 1). Moreover, HFat-fed mice present decreased relative abundance of n-3 and n-6 polyunsaturated

fatty acids (PUFAs), when compared to Chow-fed mice and HFruet-fed mice (Table 1). The decrease in n-3 PUFA is mainly attributed to a decrease in docosahexaenoic acid (DHA; C22:6 n3) and α -linolenic acid (C18:3n3), while the decrease in n-6 PUFA is mainly due to a decrease in linoleic acid (C18:2n6).

High-fat and high-fructose diets differentially affect muscle metabolome

Skeletal muscle is a major organ of glucose uptake, storage, and usage. The muscle can store glucose in the form of

TABLE 1 Fatty acid composition of liver tissue obtained from normal chow diet (Chow), high-fat diet (HFat), and high-fructose (HFru) fed male C57Bl6/J mice after 12 weeks of diet.

Fatty Acid	Chow	HFat	HFru
C10:0	0.000 ± 0.000	0.017 ± 0.003	0.000 ± 0.000
C12:0	0.141 ± 0.027	1.370 ± 0.225	0.159 ± 0.028
C14:0	0.517 ± 0.051	3.182 ± 0.272 ^a	0.494 ± 0.047 ^b
C15:0	0.090 ± 0.005	0.082 ± 0.005	0.081 ± 0.005
C16:0	24.097 ± 0.309	25.915 ± 0.225 ^a	20.880 ± 0.318 ^{a,b}
C16:1n7	2.876 ± 0.256	8.025 ± 0.280 ^a	3.004 ± 0.197 ^b
C18:0	6.801 ± 0.538	4.027 ± 0.272 ^a	7.793 ± 0.562 ^b
C18:1n9	22.877 ± 0.889	33.708 ± 1.234 ^a	29.316 ± 0.961 ^{a,b}
C18:1n7	1.917 ± 0.045	5.440 ± 0.541 ^a	2.570 ± 0.047 ^b
C18:2n6	25.679 ± 1.135	8.312 ± 0.613 ^a	19.856 ± 0.312 ^{a,b}
C18:3n3	0.623 ± 0.063	0.208 ± 0.021	0.414 ± 0.017
C20:1n9	0.236 ± 0.033	0.430 ± 0.036	0.379 ± 0.023
C20:3n6	0.497 ± 0.053	0.503 ± 0.020	0.843 ± 0.069
C20:4n6	8.167 ± 0.764	4.845 ± 0.335 ^a	8.260 ± 0.474 ^b
C22:4n6	0.197 ± 0.012	0.152 ± 0.009	0.167 ± 0.010
C22:5n6	0.121 ± 0.014	0.263 ± 0.015	0.124 ± 0.009
C22:5n3	0.299 ± 0.012	0.227 ± 0.025	0.256 ± 0.006
C22:6n3	4.863 ± 0.425	3.312 ± 0.244 ^a	5.407 ± 0.298 ^b
Σ MUFA	27.906 ± 1.134	47.597 ± 1.609 ^a	35.270 ± 1.118 ^{a,b}
Σ n3 PUFA	5.783 ± 1.134	3.745 ± 0.279 ^a	6.074 ± 0.289 ^b
Σ n6 PUFA	34.661 ± 0.958	14.074 ± 0.895 ^a	29.274 ± 0.435 ^{a,b}
Σ SFA	31.650 ± 0.622	34.585 ± 0.625 ^a	29.407 ± 0.560 ^{a,b}

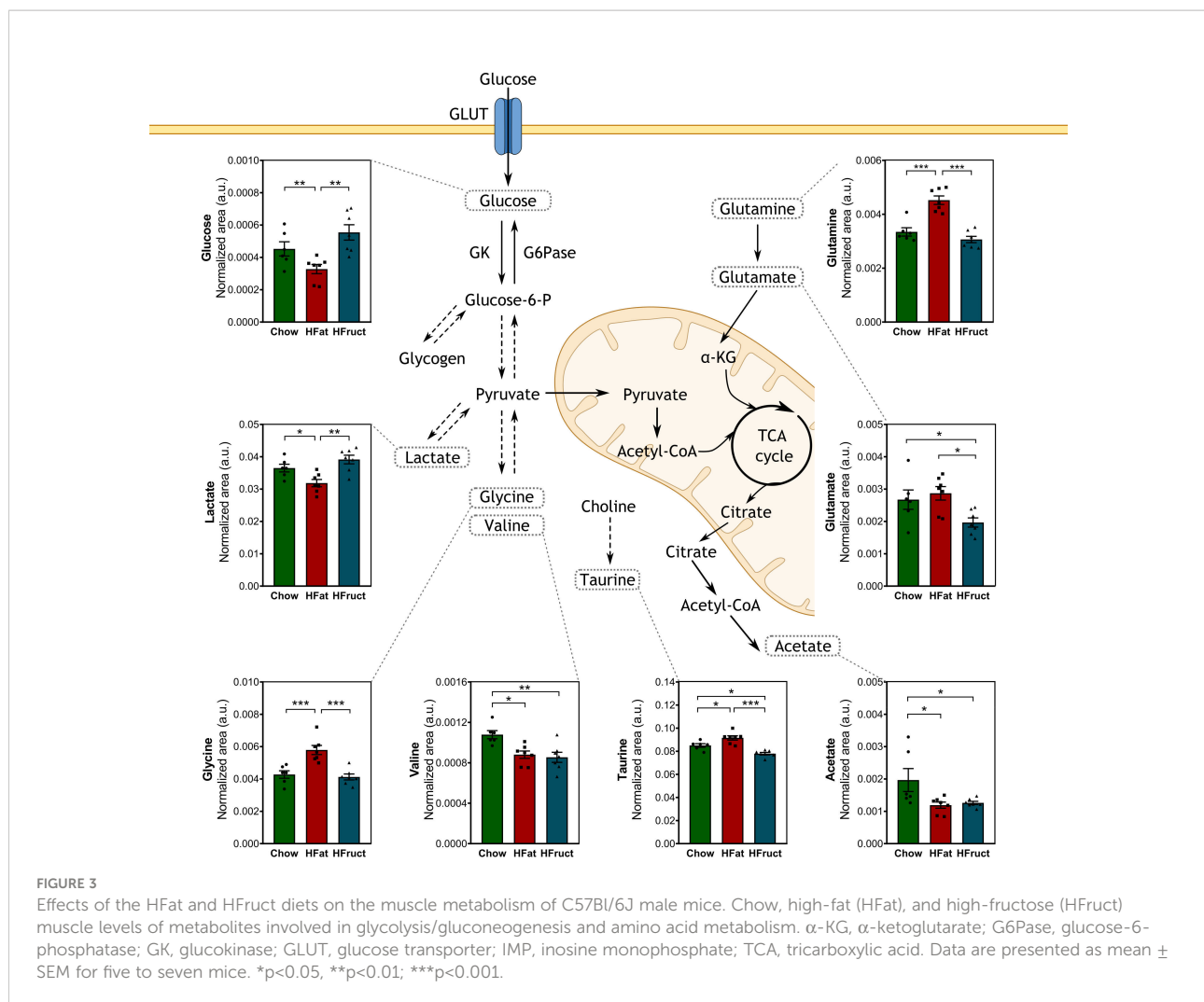
Values represent mean ± SEM for five to seven mice per experimental group. ^ap<0.05 vs. Chow; ^bp<0.05 vs. HFat. Monounsaturated fatty acids (MUFAs) correspond to C16:1n7, C18:1n9, C18:1n7, and C20:1n9. n-3 polyunsaturated fatty acids (PUFAs) correspond to C18:3n3, C22:5n3, and C22:6n3; n-6 PUFA correspond to C18:2n6, C20:3n6, C20:4n6, C22:4n6, and C22:5n6. Saturated fatty acids (SFAs) correspond to C10:0, C12:0, C14:0, C15:0, C16:0, and C18:0.

glycogen, which is crucial for the rapid initiation of energy production even when glucose is not readily available (29). Therefore, we evaluated the muscle intracellular polar metabolites after 12 weeks of HFat or HFru feeding. Muscular glucose levels were decreased in HFat-diet fed mice, compared with both Chow and HFru-diet-fed mice (Figure 2A). Lactate, which may be converted into pyruvate, was also decreased in HFat-diet-fed mice compared with both Chow- and HFru-diet-fed mice. In the need of substrate, fatty acids stored as triglycerides or amino acids may be metabolized (30). In fact, dietary changes had the major impact in amino acids levels. Glycine and glutamine were increased in HFat-diet-fed mice compared to the other diets, which may promote and contribute for protein synthesis (31). Both dietary interventions caused a decrease in valine, whose metabolism produces ammonia by-products that may participate in the conversion of glutamate to glutamine (32), but only HFru led to decreased levels of glutamate, when compared to Chow-diet-fed mice. A graphical diagram with the most affected metabolites is depicted in Figure 3, along with the graphs for each metabolite, and a heat map is depicted in Supplementary Figure 2A, and the most affected pathways in the muscle by

HFat (Supplementary Figure 2B) or HFru feeding (Supplementary Figure 2C).

Epididymal white adipose tissue metabolome is less affected by high-fat and high-fructose feeding than the liver and muscle

As a source of energy substrates, WAT responds to variations in the body's nutritional status and energy demand (33). Herein, we observed that HFat feeding for 12 weeks led to increased acetate levels (Figure 4E), which might indicate suppressed lipolysis (34), and decreased glycerophosphocholine (Figure 4B) when compared to Chow. Moreover, HFat-fed mice presented decreased creatine, a metabolite known for stimulating energy expenditure (35) (Figure 4D), and increased taurine (Figure 4A), when compared to HFru-fed mice, all pointing towards an obesogenic mechanism (36). On the other hand, HFru animals had decreased succinate, when compared to Chow-fed mice (Figure 4C). No significant differences were observed in formate levels (Figure 4F). A heat map with analyzed metabolites is depicted in Supplementary Figure 3A



and the most affected pathways in WAT by HFat (Supplementary Figure 3B).

Brown adipose tissue metabolome is modulated by high-fat or high-fructose feeding

Although it has been disregarded for years, studies about the presence of BAT in adults and the discovery of its crosstalk with important metabolic organs, namely, the muscle, has brought BAT to the spotlight (37). The BAT metabolome was assessed, and the graphical diagram in Figure 5 discloses the most affected metabolites, along with the graphs for each metabolite, and a heat map is depicted in Supplementary Figure 4A and the most affected pathways in BAT by HFat (Supplementary Figure 4B) or HFruet feeding (Supplementary Figure 4C). HFruet led to an increase in betaine, taurine, glutamine, and leucine. In contrast, the same diet led to a decrease in 3-hydroxybutyrate when

compared to Chow-diet-fed mice (Figure 5). On the other hand, HFat diet led to a decrease in glutathione (GSH), which was already reported to be inversely correlated with the activation of thermogenesis, the hallmark function of BAT (38). Moreover, HFat feeding resulted in decreased levels of glycerol, when compared to Chow-diet-fed mice. On the other hand, HFat caused an increase in glutamine and acetate compared with Chow diet, and the latter was already associated with upregulation of mitochondrial biogenesis, contributing to increased thermogenesis (39).

HFat decreases n-6 PUFA while HFruet diets increase MUFA in brown adipose tissue

BAT fatty acid methyl esters levels were measured upon HFat and HFruet feeding for 12 weeks. We observed that HFat diet leads to an increase in relative abundance of saturated fatty

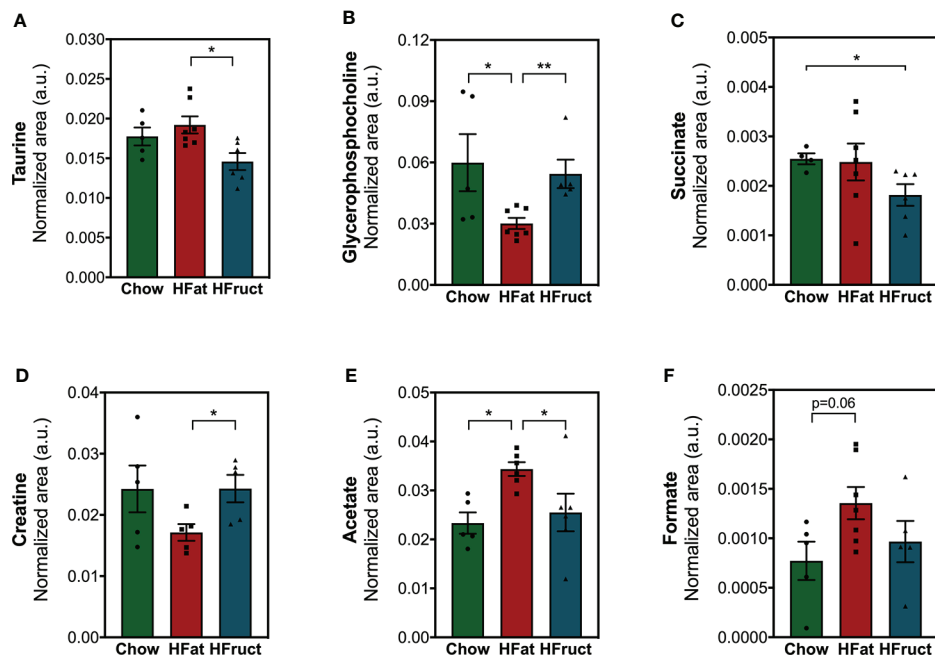


FIGURE 4

Effects of the HFat and HFruet diets on the epididymal white adipose tissue (WAT) metabolism of C57Bl/6J male mice. (A) Taurine; (B) glycerophosphocholine; (C) succinate; (D) creatine; (E) acetate; (F) formate relative areas in WAT after 12 weeks of normal chow (Chow), high-fat (HFat), or high-fructose (HFruet) feeding. Data are presented as mean \pm SEM for four to seven mice. * $p < 0.05$, ** $p < 0.01$.

acids (SFAs; 44.27 ± 0.45) when compared to Chow-fed mice and HFruet-fed mice (25.58 ± 0.75 and 23.62 ± 0.96 , respectively; Table 2). On the contrary, n-6 PUFA were decreased in HFat (7.95 ± 0.13) fed mice, when compared to both Chow- (24.65 ± 1.72) and HFruet (19.63 ± 0.42)-fed mice, mainly due to a decrease in linoleic acid (C18:2n6). MUFA were increased in HFruet-fed mice (56.10 ± 0.82) in comparison with both Chow- (48.82 ± 1.11) and HFat (47.45 ± 0.48)-fed mice, reflecting an increase in elaidic acid (C18:1n9).

Discussion

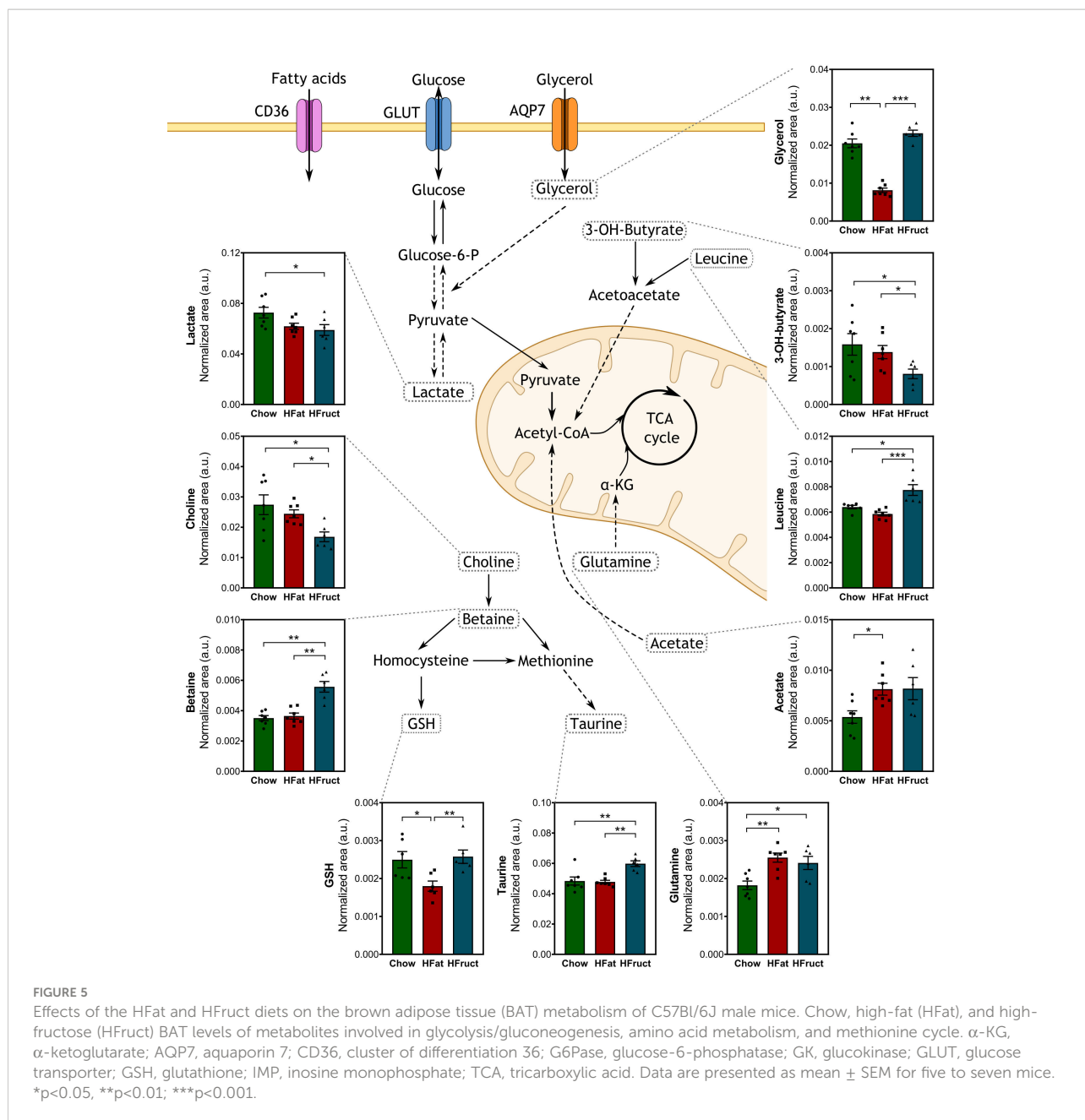
The sedentary lifestyle and poor nutritional habits have led to an increase in the prevalence of metabolic disorders, such as obesity, T2DM and NAFLD. Importantly, the increased consumption of ultra-processed food resulted in increased intake of simple carbohydrates and saturated fat (40). Although it is already known that the enrichment in lipids and in carbohydrates, particularly fructose, has different pathophysiological effects, the consequence of these specific components of the diet on the metabolome of important metabolic organs such as the liver, muscle, and adipose tissue depots remains to be fully understood.

HFat diet, alone or combined with sucrose as is the case of the present study (D12331, ResearchDiets), is known to lead to

obesity and insulin resistance in mice, originating a similar metabolic imbalance to what is observed in humans (41–43). On the other hand, fructose alone does not cause a significant increase in body weight (44). This effect is also seen in humans, and, in comparison with glucose, fructose has less effects on body weight gain (45), despite fructose deleterious effects in inflammatory processes (46).

The current study confirmed that, at 18 weeks of age and after 12 weeks of feeding, HFat-diet-fed mice had higher caloric intake, body weight, and hyperglycemia than Chow-diet-fed mice. Moreover, HFat-diet-fed mice were glucose intolerant and insulin resistant. Conversely, HFruet-diet-fed mice presented lower body weight gain than the Chow group and normal glucose tolerance. Although these animals had a decreased food intake, compared to the Chow group, the caloric intake was similar. Both food, water, and caloric intake results are supported by previous studies, although with a slightly different percentage of fructose (44, 47).

Nutritional imbalances promoting ectopic lipid accumulation are particularly striking in the liver (48, 49). Our results are in line with what is already described in the literature (50, 51). Indeed, HFat mice developed NAFL, with increased triglycerides and cholesterol. HFruet-diet-fed mice developed mild hepatic degeneration mainly in periportal areas. This impact of an HFruet diet on liver histology may be due to the activation of a lipogenic pathway and the absence of a regulatory



mechanism of fructose metabolism, contrarily to what happens with glucose (52, 53). Consequently, fructolysis will continue to occur, even when glycolysis is inhibited due to positive cellular energy balance. In fact, this effect was already been observed in studies with as low as 10% of fructose in drinking water (50). A proper glucose usage depends on a functional insulin signaling pathway. Indeed, hepatic insulin signaling was severely affected by both diets. A profound decrease in Akt phosphorylation at both phosphorylation sites was found, demonstrating that these animals are insulin resistant due to an impairment of the insulin signaling pathway, upstream of Akt, but downstream of the InsR (54). These results are supported by previous studies where

insulin signaling is severely affected by fructose intake, namely, through a decrease in Akt phosphorylation (53, 55).

The liver is the most important metabolic organ, regulating carbohydrate, lipid, and protein metabolism (56). While in the fed state, liver takes up glucose that is either stored as glycogen or converted into fatty acids; in the fasted state, liver produces and releases glucose through glycogenolysis and gluconeogenesis (56). Subsequently, substrates as glucose and triglycerides go into the bloodstream and are metabolized by peripheral organs. Adipose tissue, in turn, releases non-esterified fatty acids and glycerol. Together with alanine and lactate, which are released by the muscle, these metabolites are used as precursors for

TABLE 2 Fatty acid composition of brown adipose tissue (BAT) obtained from normal chow diet (Chow), high-fat diet (HFat), and high-fructose (HFru) fed male C57Bl6/J mice after 12 weeks of diet.

Fatty Acid	Chow	HFat	HFru
C10:0	0.013 ± 0.005	0.210 ± 0.013	0.023 ± 0.012
C12:0	0.390 ± 0.155	9.767 ± 0.330 ^a	1.010 ± 0.384 ^b
C14:0	1.896 ± 0.137	11.261 ± 0.141 ^a	2.137 ± 0.358 ^b
C15:0	0.074 ± 0.004	0.066 ± 0.003	0.046 ± 0.008
C16:0	18.601 ± 0.761	19.777 ± 0.134 ^a	14.823 ± 0.461 ^{a,b}
C16:1n7	5.709 ± 0.560	9.066 ± 0.279 ^a	4.369 ± 0.213 ^{a,b}
C18:0	4.314 ± 0.100	2.947 ± 0.111 ^a	4.804 ± 0.158 ^b
C18:1n9	39.277 ± 0.550	35.859 ± 0.474 ^a	47.856 ± 0.854 ^{a,b}
C18:1n7	2.976 ± 0.165	2.109 ± 0.049	2.853 ± 0.088
C18:2n6	23.689 ± 1.650	7.397 ± 0.121 ^a	18.016 ± 0.403 ^{a,b}
C18:3n3	0.569 ± 0.027	0.211 ± 0.006	0.326 ± 0.019
C20:0	0.256 ± 0.028	0.239 ± 0.019	0.727 ± 0.053
C20:1n9	0.861 ± 0.041	0.417 ± 0.013	1.027 ± 0.042
C20:3n6	0.184 ± 0.008	0.084 ± 0.003	0.186 ± 0.009
C20:4n6	0.703 ± 0.060	0.433 ± 0.025	1.369 ± 0.104
C22:0	0.030 ± 0.009	0.000 ± 0.000	0.050 ± 0.012
C22:4n6	0.051 ± 0.010	0.019 ± 0.003	0.036 ± 0.007
C22:5n6	0.024 ± 0.005	0.020 ± 0.004	0.023 ± 0.004
C22:5n3	0.046 ± 0.009	0.024 ± 0.003	0.027 ± 0.005
C22:6n3	0.336 ± 0.023	0.097 ± 0.006	0.297 ± 0.009
Σ MUFA	48.823 ± 1.112	47.449 ± 0.479	56.104 ± 0.823 ^{a,b}
Σ n3 PUFA	0.950 ± 0.047	0.334 ± 0.005 ^a	0.649 ± 0.018 ^{a,b}
Σ n6 PUFA	24.650 ± 1.719	7.951 ± 0.134 ^a	19.630 ± 0.424 ^{a,b}
Σ SFA	25.577 ± 0.750	44.267 ± 0.447 ^a	23.617 ± 0.961 ^b

Values represent mean ± SEM for five to seven mice per experimental group. ^ap<0.05 vs. Chow; ^bp<0.05 vs. HFat. Monounsaturated fatty acids (MUFAs) correspond to C16:1n7, C18:1n9, C18:1n7, and C20:1n9. n-3 polyunsaturated fatty acids (PUFA) correspond to C18:3n3, C22:5n3, and C22:6n3; n-6 PUFA correspond to C18:2n6, C20:3n6, C20:4n6, C22:4n6, and C22:5n6. Saturated fatty acids (SFAs) correspond to C10:0, C12:0, C14:0, C15:0, C16:0, C18:0, C20:0, and C22:0.

gluconeogenesis. Hepatic glycogen levels were decreased in HFat-diet-fed mice. Interestingly, glucokinase expression levels were increased in the liver, while G6Pase levels were unchanged. These results point towards a metabolic dysregulation; as in the fasted state, it is expected that glucokinase transcription decreases in favor of G6Pase expression. In addition, glycerate-3-phosphate produced during glycolysis can be converted to serine, which is interconvertible with glycine. While serine was decreased in the liver of HFat-diet-fed mice, glycine was increased. In fact, decreased hepatic levels of serine, due to a downregulation of phosphoglycerate dehydrogenase, contribute to the development of fatty liver disease (57). One of the pathological features of fatty liver disease is hepatocyte swelling, which was observed in our study in HFat-diet-fed mice. Indeed, glutamine, a potent osmoregulator that contributes to cell swelling (28), was increased in HFat-diet-fed mice compared to Chow-fed mice. Moreover, glutamine, is known for promoting stimulation of canalicular bile salt excretion (58). On the other hand, glycine is involved in the enterohepatic cycle of bile acids, key players in lipid absorption and regulation of cholesterol homeostasis (27), which were also

increased in the HFat group. Aside from glycine, taurine, which is also conjugated with cholesterol for the synthesis of bile acids, was increased in the liver of HFat-diet-fed mice. All these results point towards an increased production of bile acids. In fact, bile acids are crucial for an effective digestion of lipids (59). As these amino acids and cholesterol were increased only in HFat-diet-fed mice, it suggests a possible response to the increased lipid intake. Consistently, we also observe an increase in hepatic Srebp2 and Scd1 expression, suggesting that the lipogenic pathway may be active as a response to increased levels of hepatic fatty acid levels. Moreover, glycerol was increased in the liver of HFat-diet-fed mice, pointing towards an increase in adipose tissue lipolysis, which goes in line with previous studies in adipocytes (60). Additionally, dietary composition had repercussions on hepatic lipid composition, and we observed an increase in hepatic SFA in HFat-fed mice compared to Chow. SFAs are potent lipotoxic species and induce apoptosis and proinflammatory pathways through several mechanisms (61). Although this increase was not so prominent, there was also a decrease in PUFA, known to play a protective role against cell injury by clearing fat from hepatocytes and improving liver

histology and lipid profile in patients with NASH (62). Altogether, this imbalance in the lipid species might contribute to NAFL development in the HFat group. On the other hand, the HFruet group also presents a decrease in hepatic glycogen levels, without changes in the expression of any of the analyzed glucose- and lipid-metabolism-related genes. However, there was an increase in MUFA and a decrease in n-6 PUFA in comparison with Chow. In fact, there have been contradictory results in the literature regarding MUFA levels and *Scd1* mRNA expression (63); however, the animals were fed with 60% (w/v) fructose for a longer period than in the present study, which indicates that the effects of fructose on the activation of lipogenic pathways are time and dose dependent. Interestingly, we found an increase in alanine levels, in concurrence with the data obtained in a recent study with HFruet-fed rats (64). This increase in alanine levels may be a consequence of an increase in the release of alanine from the muscle that is then delivered to the liver through Cahill cycle or to its conversion from pyruvate in the liver.

The skeletal muscle is a major site for glucose metabolism. Insulin resistance in the muscle is known to cause glycogen depletion, lipid accumulation, impairment of the tissue's normal functions, ultimately leading to sarcopenia (29). Muscle stores glucose in the form of glycogen, which facilitates the rapid initiation of energy production for contraction, even when glucose is not readily available from circulation (29). In this study, HFat diet promoted a decrease in glucose and lactate pools in the muscle, pointing towards the use of other substrates to obtain energy. In the need for other substrates, amino acids may be metabolized. Skeletal muscles are the most relevant site of glutamine stock, synthesis, and release (65). In this study, glutamine levels were increased in HFat-fed mice, and glutamate levels remained similar to the levels detected in the muscle of Chow-diet-fed mice. Glutamate levels can be used to produce glutamine that will be then delivered to the liver where it may have several functions (65, 66). Indeed, and as there was no glycogen pool in the liver, gluconeogenesis may use glutamine as a substrate for glucose production after an overnight fasting (32), as was the case of the present study. On the contrary, HFruet diet promoted a decrease in muscular glutamate levels, which might negatively affect glutathione synthesis and/or purine nucleotide cycle (67). Moreover, a decrease in valine was observed in both HFat- and HFruet-fed groups. Valine is used to obtain energy with the resulting ammonia by-products participating in the conversion of glutamate to glutamine, thus sustaining the previously mentioned hypothesis. Although it has already been described that diet-induced obese animals have a decrease in branched-chain amino acids (BCAAs) (68), there are studies describing a positive correlation between valine circulating levels and insulin resistance in men (69, 70).

WAT has a crucial role for lipid homeostasis, namely, by regulating triglyceride levels, and for fatty acid availability by lipolysis, also generating substrates for energy metabolism *via*

β -oxidation. In fact, we observed an increase in the WAT levels of acetate in HFat-fed mice compared to Chow, which indicates increased β -oxidation (71). On the contrary, creatine was decreased in HFat-fed mice compared to HFruet-fed mice. As this metabolite enhances energy expenditure (35), the finding goes in accordance with the larger fat depots in this group. Although taurine promotes thermogenesis in the BAT and muscle, it does not have the same effect in WAT (72), which was also not observed in the present study. In fact, taurine supplementation was shown to prevent obesity in female mice after 18 weeks of high-fat feeding (36). In this study, male mice fed with HFat diet for 12 weeks presented no differences in taurine compared to the Chow group, which might indicate that decreases in taurine may be more noticeable in females or only appear with prolonged HFat feeding.

Organ crosstalk is mediated by signaling factors and ensures whole-body metabolic homeostasis. However, in case of disease or metabolic dysfunction, metabolic impairment in one organ will lead to dysregulation of others. Although this is known, the interplay and metabolic crosstalk between the different organs remain obscure. In recent years, BAT was rediscovered, and very recently, the existence of a crosstalk with the liver and the muscle was unveiled (73). HFat diet led to a decrease in GSH levels in the BAT compared with both Chow and HFruet diets. GSH was already reported to be inversely correlated with the activation of thermogenesis in white adipocytes due to its action on forkhead box O1 (74). Consequently, decreased GSH levels might have the same effect in BAT and increase thermogenesis in the BAT of HFat-diet-fed mice (38). Moreover, HFat-diet-fed mice had increased levels of glutamine and acetate in BAT. Acetate upregulates mitochondrial biogenesis, which is the key organelle for thermogenesis (39). Importantly, HFruet feeding led to an increase in betaine and taurine, probably at the expense of decreased choline. In fact, betaine protects against fructose-induced inflammation in astrocytes (75). HFruet-diet-fed animals also presented increased leucine. This amino acid is an activator of the mammalian target of rapamycin (mTOR) pathway, leading to reduced thermogenesis (76, 77). Moreover, the levels of 3-OH-butyrate, considered an alternative carbon source for thermogenesis (78), were decreased in HFruet-fed mice. Thus, high-fat feeding seems to be an activator of thermogenesis, while HFruet leads to a decrease in this process. Moreover, it was already reported that in HFat conditions, BAT functions largely like WAT in its role as a depot for excess energy (79). In these cases, adipocytes suffer a remodeling due to its storage needs and, consequently, the need of the membrane to be more fluid (80). In fact, we observed a completely different fatty acid distribution in HFat-fed mice compared to both Chow- and HFruet-fed mice that were lean. This difference might represent the need of the adipocytes to remodel and be able to store more fat.

In summary, our data provide novel evidence that, aside from the extensively described effects of high-fat and high-

fructose diets on glucose and insulin homeostasis, these diets differentially and significantly affect liver, muscle, WAT, and BAT metabolic profiles. Interestingly, our data suggests a crosstalk between the liver, muscle, and BAT, specifically through alanine, glutamine, and lactate.

Data availability statement

The raw data supporting the conclusions of this article will be made available by the authors, without undue reservation.

Ethics statement

The animal study was reviewed and approved by DGAV - Portuguese General Directorate of Food and Veterinary Medicine and by NOVA Medical School Ethics Committee.

Author contributions

MJM: experimental work, animal studies, data analysis and interpretation, and writing of the manuscript. IS-L: experimental work, animal studies, and data analysis and interpretation. IJ: NMR and data analysis. JFR: data interpretation. MGA: conceptualization, data interpretation, and writing of manuscript. MPM: conceptualization, supervision, data interpretation, and writing of the manuscript. All authors read and agree with the final version of the manuscript.

Funding

This work was supported by “Fundação para a Ciência e a Tecnologia”—FCT MJM (PD/BD/114256/2016), MPM (PTDC/BIM-MET/4265/2014 and PTDC/MEC-MET/29314/2017), MGA (PTDC/BIM-MET/4712/2014), iNOVA4Health (UIDB/Multi/04462/2020), by the European Commission Marie Skłodowska-Curie Action H2020 (mtFOIE GRAS, grant agreement n. 734719), by the Sociedade Portuguesa de

Diabetologia, and by the research infrastructure CONGENTO, project LISBOA-01-0145-FEDER-022170, co-financed by Lisboa Regional Operational Programme (Lisboa2020), under the PORTUGAL 2020 Partnership Agreement, through the European Regional Development Fund and by Fundação para a Ciência e Tecnologia (Portugal). NMR data were collected at the UC-NMR facility which is supported in part by FEDER – European Regional Development Fund through the COMPETE Programme (Operational Programme for Competitiveness) and by National Funds through FCT – Fundação para a Ciência e a Tecnologia (Portuguese Foundation for Science and Technology) through grants REEQ/481/QUI/2006, RECI/QEQ-QFI/0168/2012, CENTRO-07-CT62-FEDER-002012, and Rede Nacional de Ressonância Magnética Nuclear (RNRMN).

Conflict of interest

The authors declare that the research was conducted in the absence of any commercial or financial relationships that could be construed as a potential conflict of interest.

The reviewer RS declared a shared affiliation with the author MA to the handling editor at the time of review.

Publisher's note

All claims expressed in this article are solely those of the authors and do not necessarily represent those of their affiliated organizations, or those of the publisher, the editors and the reviewers. Any product that may be evaluated in this article, or claim that may be made by its manufacturer, is not guaranteed or endorsed by the publisher.

Supplementary material

The Supplementary Material for this article can be found online at: <https://www.frontiersin.org/articles/10.3389/fendo.2022.898471/full#supplementary-material>

References

1. Fan J-G, Kim S-U, Wong VW-S. New trends on obesity and NAFLD in Asia. *J Hepatol* (2017) 67(4):862–73. doi: 10.1016/j.jhep.2017.06.003
2. NCD Risk Factor Collaboration. Trends in adult body-mass index in 200 countries from 1975 to 2014: a pooled analysis of 1698 population-based measurement studies with 19.2 million participants. *Lancet* (2016) 387(10026):1377–96. doi: 10.1016/S0140-6736(16)30054-X
3. Grarup N, Sandholt CH, Hansen T, Pedersen O. Genetic susceptibility to type 2 diabetes and obesity: from genome-wide association studies to rare variants and beyond. *Diabetologia* (2014) 57(8):1528–41. doi: 10.1007/s00125-014-3270-4
4. Eng JM, Estall JL. Diet-induced models of non-alcoholic fatty liver disease: Food for thought on sugar, fat, and cholesterol. *Cells* (2021) 10(7):1805. doi: 10.3390/cells10071805
5. Stott NL, Marino JS. High fat rodent models of type 2 diabetes: From rodent to human. *Nutrients* (2020) 12(12):3650. doi: 10.3390/nu12123650
6. Nonaka H, Ohue-Kitano R, Masujima Y, Igarashi M, Kimura I. Dietary medium-chain triglyceride decanoate affects glucose homeostasis through GPR84-mediated GLP-1 secretion in mice. *Front Nutr* (2022) 9:848450. doi: 10.3389/fnut.2022.848450

7. Tchernof A, Després J-P. Pathophysiology of human visceral obesity: An update. *Physiol Rev* (2013) 93(1):359. doi: 10.1152/physrev.00033.2011
8. Merino J. Precision nutrition in diabetes: when population-based dietary advice gets personal. *Diabetologia* (2022) Ahead of print. doi: 10.1007/s00125-022-05721-6
9. Pascot A, Lemieux I, Prud'homme D, Tremblay A, Nadeau A, Couillard C, et al. Reduced HDL particle size as an additional feature of the atherogenic dyslipidemia of abdominal obesity. *J Lipid Res* (2001) 42(12):2007–14. doi: 10.1016/S0022-2275(20)31529-7
10. Muzurović E, Peng CC-H, Belanger MJ, Sanoudou D, Mikhailidis DP, Mantzoros CS. Nonalcoholic fatty liver disease and cardiovascular disease: a review of shared cardiometabolic risk factors. *Hypertension* (2022) 79(7):1319–26. doi: 10.1161/HYPERTENSIONAHA.122.17982
11. Cusi K, Isaacs S, Barb D, Basu R, Caprio S, Garvey WT, et al. American Association of clinical endocrinology clinical practice guideline for the diagnosis and management of nonalcoholic fatty liver disease in primary care and endocrinology clinical settings: Co-sponsored by the American association for the study of liver diseases (AASLD). *Endocr Pract* (2022) 28(5):528–62. doi: 10.1016/j.eprac.2022.03.010
12. Bellentani S. The epidemiology of non-alcoholic fatty liver disease. *Liver Int* (2017) 37(Suppl 1):81–4. doi: 10.1111/liv.13299
13. Bosserhoff A, Hellerbrand C. Obesity and fatty liver are 'grease' for the machinery of hepatic fibrosis. *Digest Dis (Basel Switzerland)* (2011) 29(4):377–83. doi: 10.1159/000329800
14. Scheja L, Heeren J. Metabolic interplay between white, beige, brown adipocytes and the liver. *J Hepatol* (2016) 64(5):1176–86. doi: 10.1016/j.jhep.2016.01.025
15. De Bandt JP, Jegatheesan P, Tennoune-El-Hafaa N. Muscle loss in chronic liver diseases: The example of nonalcoholic liver disease. *Nutrients* (2018) 10(9):1195. doi: 10.3390/nu10091195
16. Andrikopoulos S, Blair AR, Deluca N, Fam BC, Proietto J. Evaluating the glucose tolerance test in mice. *Am J Physiol Endocrinol Metab* (2008) 295(6):E1323–32. doi: 10.1152/ajpendo.90617.2008
17. Matyash V, Liebisch G, Kurzchalia TV, Shevchenko A, Schwudke D. Lipid extraction by methyl-tert-butyl ether for high-throughput lipidomics. *J Lipid Res* (2008) 49(5):1137–46. doi: 10.1194/jlr.D700041-JLR200
18. Pfaffl MW. A new mathematical model for relative quantification in real-time RT-PCR. *Nucleic Acids Res* (2001) 29(9):e45–5. doi: 10.1093/nar/29.9.e45
19. Wishart DS, Tzur D, Knox C, Eisner R, Guo AC, Young N, et al. HMDB: the human metabolome database. *Nucleic Acids Res* (2007) 35(suppl_1):D521–6. doi: 10.1093/nar/gk923
20. Sumner LW, Amberg A, Barrett D, Beale MH, Beger R, Daykin CA, et al. Proposed minimum reporting standards for chemical analysis chemical analysis working group (CAWG) metabolomics standards initiative (MSI). *Metabolomics* (2007) 3(3):211–21. doi: 10.1007/s11306-007-0082-2
21. Savorani F, Tomasi G, Engelsen SB. Icoshift: A versatile tool for the rapid alignment of 1D NMR spectra. *J Magn Reson* (2010) 202(2):190–202. doi: 10.1016/j.jmr.2009.11.012
22. Xia J, Wishart DS. Using MetaboAnalyst 3.0 for comprehensive metabolomics data analysis. *Curr Protoc Bioinf* (2016) 55:14.10.11–14.10.91. doi: 10.1002/cpbi.11
23. Patti M-E. Gene expression in humans with diabetes and prediabetes: what have we learned about diabetes pathophysiology? *Curr Opin Clin Nutr Metab Care* (2004) 7(4):383–90. doi: 10.1097/01.mco.0000134359.23288.72
24. Patsouris D, Mandar S, Voshol PJ, Escher P, Tan NS, Havekes LM, et al. PPAR α governs glycerol metabolism. *J Clin Invest* (2004) 114(1):94–103. doi: 10.1172/JCI200420468
25. Sivanesan S, Taylor A, Zhang J, Bakovic M. Betaine and choline improve lipid homeostasis in obesity by participation in mitochondrial oxidative demethylation. *Front Nutr* (2018) 5. doi: 10.3389/fnut.2018.00061
26. Abdul-Ghani MA, Matsuda M, Balas B, DeFronzo RA. Muscle and liver insulin resistance indexes derived from the oral glucose tolerance test. *Diabetes Care* (2007) 30(1):89–94. doi: 10.2337/dc06-1519
27. Alves A, Bassot A, Bulteau AL, Pirola L, Morio B. Glycine metabolism and its alterations in obesity and metabolic diseases. *Nutrients* (2019) 11(6):1356. doi: 10.3390/nu11061356
28. Häussinger D, Graf D, Weiergräber OH. Glutamine and cell signaling in liver. *J Nutr* (2001) 131(9 Suppl):2509S–2514S; discussion 2523S–2504S. doi: 10.1093/jn/131.9.2509S
29. Racheck LI. Free fatty acids and skeletal muscle insulin resistance. *Prog Mol Biol Transl Sci* (2014) 121:267–92. doi: 10.1016/B978-0-12-800101-1.00008-9
30. Moro T, Ebert SM, Adams CM, Rasmussen BB. Amino acid sensing in skeletal muscle. *Trends Endocrinol Metab* (2016) 27(11):796–806. doi: 10.1016/j.tem.2016.06.010
31. Jepson MM, Bates PC, Broadbent P, Pell JM, Millward DJ. Relationship between glutamine concentration and protein synthesis in rat skeletal muscle. *Am J Physiol Endocrinol Metab* (1988) 255(2):E166–72. doi: 10.1152/ajpendo.1988.255.2.E166
32. Stumvoll M, Perriello G, Meyer C, Gerich J. Role of glutamine in human carbohydrate metabolism in kidney and other tissues. *Kidney Int* (1999) 55(3):778–92. doi: 10.1046/j.1523-1755.1999.055003778.x
33. Wronska A, Kmiec Z. Structural and biochemical characteristics of various white adipose tissue depots. *Acta Physiol (Oxf)* (2012) 205(2):194–208. doi: 10.1111/j.1748-1716.2012.02409.x
34. Sahuri-Arisoylu M, Brody LP, Parkinson JR, Parkes H, Navaratnam N, Miller AD, et al. Reprogramming of hepatic fat accumulation and 'browning' of adipose tissue by the short-chain fatty acid acetate. *Int J Obes (Lond)* (2016) 40(6):955–63. doi: 10.1038/ijo.2016.23
35. Kazak L, Chouchani ET, Lu GZ, Jedrychowski MP, Bare CJ, Mina AI, et al. Genetic depletion of adipocyte creatine metabolism inhibits diet-induced thermogenesis and drives obesity. *Cell Metab* (2017) 26(4):660–71.e663. doi: 10.1016/j.cmet.2017.08.009
36. Tsuboyama-Kasaoka N, Shozawa C, Sano K, Kamei Y, Kasaoka S, Hosokawa Y, et al. Taurine (2-aminoethanesulfonic acid) deficiency creates a adipose circle promoting obesity. *Endocrinology* (2006) 147(7):3276–84. doi: 10.1210/en.2005-1007
37. Cypess AM. A new connection between muscle and brown fat. *J Pediatr* (2011) 158(5):696–8. doi: 10.1016/j.jpeds.2011.01.001
38. Mercer SW, Trayhurn P. Effect of high fat diets on the thermogenic activity of brown adipose tissue in cold-acclimated mice. *J Nutr* (1984) 114(6):1151–8. doi: 10.1093/jn/114.6.1151
39. Hu J, Kyrou I, Tan BK, Dimitriadis GK, Ramanjaneya M, Tripathi G, et al. Short-chain fatty acid acetate stimulates adipogenesis and mitochondrial biogenesis via GPR43 in brown adipocytes. *Endocrinology* (2016) 157(5):1881–94. doi: 10.1210/en.2015-1944
40. Rippe JM, Angelopoulos TJ. Sucrose, high-fructose corn syrup, and fructose, their metabolism and potential health effects: what do we really know? *Adv Nutr* (2013) 4(2):236–45. doi: 10.3945/an.112.002824
41. Wang ZQ, Zhang XH, Yu Y, Poulev A, Ribnicky D, Floyd ZE, et al. Bioactives from bitter melon enhance insulin signaling and modulate acyl carnitine content in skeletal muscle in high-fat diet-fed mice. *J Nutr Biochem* (2011) 22(11):1064–73. doi: 10.1016/j.jnutbio.2010.09.004
42. Small L, Brandon AE, Turner N, Cooney GJ. Modeling insulin resistance in rodents by alterations in diet: what have high-fat and high-calorie diets revealed? *Am J Physiol Endocrinol Metab* (2018) 314(3):E251–e265. doi: 10.1152/ajpendo.00337.2017
43. Surwit RS, Feinglos MN, Rodin J, Sutherland A, Petro AE, Opara EC, et al. Differential effects of fat and sucrose on the development of obesity and diabetes in C57BL/6J and A/J mice. *Metab: Clin Exp* (1995) 44(5):645–51. doi: 10.1016/0026-0495(95)90123-X
44. Bergheim I, Weber S, Vos M, Krämer S, Volynets V, Kaserouni S, et al. Antibiotics protect against fructose-induced hepatic lipid accumulation in mice: Role of endotoxin. *J Hepatol* (2008) 48(6):983–92. doi: 10.1016/j.jhep.2008.01.035
45. Sevenpiper JL, de Souza RJ, Cozma AI, Chiavaroli L, Ha V, Mirrahimi A. Fructose vs. glucose and metabolism: do the metabolic differences matter? *Curr Opin Lipidol* (2014) 25(1):8–19. doi: 10.1097/MOL.0000000000000042
46. Jegatheesan P, De Bandt J-P. Fructose and NAFLD: The multifaceted aspects of fructose metabolism. *Nutrients* (2017) 9(3):230. doi: 10.3390/nu9030230
47. Lindqvist A, Baelemans A, Erlanson-Albertsson C. Effects of sucrose, glucose and fructose on peripheral and central appetite signals. *Regul Peptides* (2008) 150(1-3):26–32. doi: 10.1016/j.regpep.2008.06.008
48. Parry SA, Hodson L. Influence of dietary macronutrients on liver fat accumulation and metabolism. *J Invest Med Off Publ Am Fed Clin Res* (2017) 65(8):1102–15. doi: 10.1136/jim-2017-000524
49. Bony-Westphal A, Braun W, Albrecht V, Muller MJ. Determinants of ectopic liver fat in metabolic disease. *Eur J Clin Nutr* (2019) 73(2):209–14. doi: 10.1038/s41430-018-0323-7
50. Yang Y, Li J, Wei C, He Y, Cao Y, Zhang Y, et al. Amelioration of nonalcoholic fatty liver disease by swertiamarin in fructose-fed mice. *Phytomed Int J Phytother Phytopharmacol* (2019) 59:152782. doi: 10.1016/j.phymed.2018.12.005
51. Jahn D, Kircher S, Hermanns HM, Geier A. Animal models of NAFLD from a hepatologist's point of view. *Biochim Biophys Acta (BBA) Mol Basis Dis* (2019) 1865(5):943–53. doi: 10.1016/j.bbadis.2018.06.023
52. Herman MA, Samuel VT. The sweet path to metabolic demise: Fructose and lipid synthesis. *Trends Endocrinol Metab* (2016) 27(10):719–30. doi: 10.1016/j.tem.2016.06.005
53. Softic S, Gupta MK, Wang G-X, Fujisaka S, O'Neill BT, Rao TN, et al. Divergent effects of glucose and fructose on hepatic lipogenesis and insulin signaling. *J Clin Invest* (2017) 127(11):4059–74. doi: 10.1172/JCI94585

54. Guo S, Copps KD, Dong X, Park S, Cheng Z, Poci A, et al. The Irs1 branch of the insulin signaling cascade plays a dominant role in hepatic nutrient homeostasis. *Mol Cell Biol* (2009) 29(18):5070–83. doi: 10.1128/MCB.00138-09
55. Sumlu E, Bostanci A, Sadi G, Alcigir ME, Akar F. Lactobacillus plantarum improves lipogenesis and IRS-1/AKT/eNOS signalling pathway in the liver of high-fructose-fed rats. *Arch Physiol Biochem* (2020) 2020:1–9. doi: 10.1080/13813455.2020.1727527
56. Rui L. Energy metabolism in the liver. *Compr Physiol* (2014) 4(1):177–97. doi: 10.1002/cphy.c130024
57. Sim WC, Lee W, Sim H, Lee KY, Jung SH, Choi YJ, et al. et al. Downregulation of PHGDH expression and hepatic serine level contribute to the development of fatty liver disease. *Metab: Clin Exp* (2020) 102:154000. doi: 10.1016/j.metabol.2019.154000
58. Hallbrucker C, Lang F, Gerok W, Häussinger D. Cell swelling increases bile flow and taurocholate excretion into bile in isolated perfused rat liver. *Biochem J* (1992) 281(Pt 3):593–5. doi: 10.1042/bj2810593
59. McGlone ER, Bloom SR. Bile acids and the metabolic syndrome. *Ann Clin Biochem* (2019) 56(3):326–37. doi: 10.1177/0004563218817798
60. Rotondo F, Ho-Palma AC, Remesar X, Fernández-López JA, Romero M, Alemany M. Glycerol is synthesized and secreted by adipocytes to dispose of excess glucose, via glycerogenesis and increased acyl-glycerol turnover. *Sci Rep* (2017) 7(1):8983. doi: 10.1038/s41598-017-09450-4
61. Wang D, Wei Y, Pagliassotti MJ. Saturated fatty acids promote endoplasmic reticulum stress and liver injury in rats with hepatic steatosis. *Endocrinology* (2006) 147(2):943–51. doi: 10.1210/en.2005-0570
62. El-Badry AM, Graf R, Clavien PA. Omega 3 - omega 6: What is right for the liver? *J Hepatol* (2007) 47(5):718–25. doi: 10.1016/j.jhep.2007.08.005
63. Miyazaki M, Dobrzyn A, Man WC, Chu K, Sampath H, Kim H-J, et al. Stearoyl-CoA desaturase 1 gene expression is necessary for fructose-mediated induction of lipogenic gene expression by sterol regulatory element-binding protein-1c-dependent and -independent mechanisms *. *J Biol Chem* (2004) 279(24):25164–71. doi: 10.1074/jbc.M402781200
64. Morrell A, Triplet BP, Eilers BJ, Tegman M, Thompson D, Copie V, et al. Copper modulates sex-specific fructose hepatotoxicity in nonalcoholic fatty liver disease (NALFD) wistar rat models. *J Nutr Biochem* (2020) 78:108316. doi: 10.1016/j.jnutbio.2019.108316
65. Cruzat V, Rogero MM, Keane KN, Curi R, Newsholme P. Glutamine: Metabolism and immune function, supplementation and clinical translation. *Nutrients* (2018) 10(11):1564. doi: 10.3390/nu10111564
66. Häussinger D, Graf D, Weiergräuber OH. Glutamine and cell signaling in liver. *J Nutr* (2001) 131(9):2509S–14S. doi: 10.1093/jn/131.9.2509S
67. Rutten EP, Engelen MP, Schols AM, Deutz NE. Skeletal muscle glutamate metabolism in health and disease: state of the art. *Curr Opin Clin Nutr Metab Care* (2005) 8(1):41–51. doi: 10.1097/00075197-200501000-00007
68. Newgard CB. Interplay between lipids and branched-chain amino acids in development of insulin resistance. *Cell Metab* (2012) 15(5):606–14. doi: 10.1016/j.cmet.2012.01.024
69. Tai ES, Tan ML, Stevens RD, Low YL, Muehlbauer MJ, Goh DL, et al. et al. Insulin resistance is associated with a metabolic profile of altered protein metabolism in Chinese and Asian-Indian men. *Diabetologia* (2010) 53(4):757–67. doi: 10.1007/s00125-009-1637-8
70. Newgard CB, An J, Bain JR, Muehlbauer MJ, Stevens RD, Lien LF, et al. et al. A branched-chain amino acid-related metabolic signature that differentiates obese and lean humans and contributes to insulin resistance. *Cell Metab* (2009) 9(4):311–26. doi: 10.1016/j.cmet.2009.02.002
71. Yamashita H, Kaneyuki T, Tagawa K. Production of acetate in the liver and its utilization in peripheral tissues. *Biochim Biophys Acta* (2001) 1532(1-2):79–87. doi: 10.1016/S1388-1981(01)00117-2
72. Kim KS, Doss HM, Kim HJ, Yang HI. Taurine stimulates thermoregulatory genes in brown fat tissue and muscle without an influence on inguinal white fat tissue in a high-fat diet-induced obese mouse model. *Foods* (2020) 9(6):688. doi: 10.3390/foods9060688
73. Scheele C, Wolfrum C. Brown adipose crosstalk in tissue plasticity and human metabolism. *Endocr Rev* (2019) 41(1):53–65. doi: 10.1210/endo/bnz007
74. Lettieri Barbato D, Tatulli G, Maria Cannata S, Bernardini S, Aquilano K, Ciriolo MR. Glutathione decrement drives thermogenic program in adipose cells. *Sci Rep* (2015) 5(1):13091. doi: 10.1038/srep13091
75. Li JM, Ge CX, Xu MX, Wang W, Yu R, Fan CY, et al. Betaine recovers hypothalamic neural injury by inhibiting astrogliosis and inflammation in fructose-fed rats. *Mol Nutr Food Res* (2015) 59(2):189–202. doi: 10.1002/mnfr.201400307
76. Cheng Y, Meng Q, Wang C, Li H, Huang Z, Chen S, et al. Leucine deprivation decreases fat mass by stimulation of lipolysis in white adipose tissue and upregulation of uncoupling protein 1 (UCP1) in brown adipose tissue. *Diabetes* (2010) 59(1):17–25. doi: 10.2337/db09-0929
77. Wang Y, Li Z, Zhang X, Xiang X, Li Y, Mulholland MW, et al. Nesfatin-1 promotes brown adipocyte phenotype. *Sci Rep* (2016) 6(1):34747. doi: 10.1038/srep34747
78. Srivastava S, Kashiwaya Y, King MT, Baxa U, Tam J, Niu G, et al. Mitochondrial biogenesis and increased uncoupling protein 1 in brown adipose tissue of mice fed a ketone ester diet. *FASEB J* (2012) 26(6):2351–62. doi: 10.1096/fj.11-200410
79. Hageman RS, Wagener A, Hantschel C, Svenson KL, Churchill GA, Brockmann GA. High-fat diet leads to tissue-specific changes reflecting risk factors for diseases in DBA/2J mice. *Physiol Genomics* (2010) 42(1):55–66. doi: 10.1152/physiolgenomics.00072.2009
80. Pietiläinen KH, Róg T, Seppänen-Laakso T, Virtue S, Gopalacharyulu P, Tang J, et al. Association of lipidome remodeling in the adipocyte membrane with acquired obesity in humans. *PLoS Biol* (2011) 9(6):e1000623. doi: 10.1371/journal.pbio.1000623